

Optical properties of the iridescent organ of the comb-jellyfish *Beroë cucumis* (Ctenophora)

Victoria Welch,¹ Jean Pol Vigneron,^{2,*} Virginie Lousse,^{2,3} and Andrew Parker⁴

¹Department of Zoology, University of Oxford, South Park Road, Oxford, OX1 3PS, United Kingdom

²Laboratoire de Physique du Solide, Facultés Universitaires Notre-Dame de la Paix, 61 rue de Bruxelles, B-5000 Namur, Belgium

³Ginzton Laboratory, Stanford University, Stanford, California 94305, USA

⁴Department of Zoology, The Natural History Museum, Cromwell Road, London, SW7 5BD, United Kingdom

(Received 12 December 2005; revised manuscript received 12 March 2006; published 14 April 2006)

Using transmission electron microscopy, analytical modeling, and detailed numerical simulations, the iridescence observed from the comb rows of the ctenophore *Beroë cucumis* was investigated. It is shown that the changing coloration which accompanies the beating of comb rows as the animal swims can be explained by the weakly-contrasted structure of the refractive index induced by the very coherent packing of locomotory cilia. The colors arising from the narrow band-gap reflection are shown to be highly saturated and, as a function of the incidence angle, cover a wide range of the visible and ultraviolet spectrum. The high transparency of the structure at the maximal bioluminescence wavelength is also explained.

DOI: [10.1103/PhysRevE.73.041916](https://doi.org/10.1103/PhysRevE.73.041916)

PACS number(s): 42.66.-p, 42.70.Qs, 42.81.-i, 42.81.Qb

I. INTRODUCTION

Ctenophores, comb-jellies or comb-jellyfishes, are common names for marine animals of the phylum Ctenophora. All parts of their deformable body, including muscles, are transparent. The refractive index of their tissues matches nearly exactly that of the salted water in which they live, consequently they are difficult to perceive, except under intense illumination, when the irregularities of their outer membrane produce some faint light scattering. The species *Beroë cucumis* has the form of oblong ellipsoids (a “cucumber” shape) with a mouth aperture in the forward swimming direction. Eight rows of locomotory cilia run along the body of the animal (see Fig. 1). These organs are usually much more easily visible than the rest of the body surface, due to the stronger light scattering which takes place on these protrusions. Moreover, the “comb”-rows appear to be brightly colored, showing an iridescence that rainbows across the whole visible spectrum as the combs beat for locomotion. As the rest of the paper will make clear, this is not related to any bioluminescence but can be understood as selective reflection from a two-dimensional photonic-crystal.

Bioluminescence is produced by *Beroë cucumis*, and becomes noticeable in a sufficiently dark environment. Indeed bioluminescence is the general (but not universal) rule among ctenophores [1], although different species vary in their wavelength of maximal bioluminescence (e.g., [2]). The bioluminescent sources of radiation of *Beroë cucumis* are located just below the comb row, so that the light has to propagate through the comb nanostructure before emerging into the open water. The question of the selective transmission of this structure is then quite important. This paper addresses the physical mechanism for the observed comb iridescence. Reverse engineering of these organs essentially rests on transmission electron microscope pictures showing the comb ciliary structure at the submicron scale. From these

views, both the selective reflectance and the transparency properties of the iridescent organs can be addressed, using computational methods for simulating the light propagation. The reflectance and transmittance computations makes use of a state-of-the-art transfer-matrix technique which has been described elsewhere [3]. The specimens considered in this study were collected during a research cruise on the Atlantic Ocean, off the United States eastern coast, between 70° and 75° west and ranging from 35° to 42° north in latitude. In order to avoid damaging the samples, the animals were collected in the sea, by a submarine equipped with purpose-built jars with hydraulically operated lids that were closed remotely.



FIG. 1. (Color online) The ctenophore *Beroë cucumis* is a transparent marine animal which can be recognized by its ellipsoidal shape and the comb rows, which are characteristic of ctenophores and run along the length of its body. These comb rows are iridescent, with rainbow colors passing down the length of the animal as it swims. This animal typically reach sizes from 6 to 10 cm. Image courtesy of Dr. Kevin Raskoff, California State University, Monterey Bay, USA.

*Electronic address: jean-pol.vigneron@fundp.ac.be

II. SUBMICRON STRUCTURE

Previous morphological studies show that the macrocilia of the lips of a *Beroë sp.* ctenophore pack together to form a coherently parallel array [4], as was found earlier on the swimming plates of other species of ctenophores (*Mnemiopsis leidyi* and *Pleurobrachia pileus*) [5,6]. The dimensions of these cilia and their highly regular arrangement is reminiscent of the color-producing structures found within the spines [7] of the polychaete worm *Aphrodita sp.*, which is known to behave optically as a photonic crystal [8]. The wavelength selectivity of photonic-crystal surfaces, due to the appearance of directional band gaps is well known, and the periodic arrangement of cilia is a good hint as to the cause of the observed iridescence.

The visual effect associated with comb-row beating is characterized by the appearance of colors which cover a significant part of the visible spectrum. The mechanism involved in the production of this iridescence must, therefore, show a large spectral sensitivity to the geometry defined by the light source, the comb axis, and the observer.

A. Sample preparation

When compared with hard photonic structures, such as those found in the cuticle of beetles, the scales of butterflies, or the barbules of bird feathers, the iridescent organs found on a ctenophore are much more difficult to manipulate. The cilia are imbedded in tissues which lack any rigidity, and it is very difficult to extract the relevant parts.

Each comb in the combs row has a dense basal region, which can easily be detected with light microscopy. This dense region was selected for examination with transmission electron microscopy and suitable samples were prepared for observation. Short parts of the comb rows, containing 4–5 combs were removed from the animal by dissection and left overnight in a 2.5% gluteraldehyde fixative solution. The samples were then washed with a sodium cacodylate buffer solution, and were osmicated in 1% osmium tetroxide for one h in the dark. The samples were rinsed with distilled water and dehydrated in an alcohol series, then transferred to propylene oxide, and impregnated with it, before being embedded in araldite. The resulting blocks were dried for 48 h in an oven at 60 °C, trimmed with a razor blade, and 1 μm thick sections were cut with a Reichert Jung “Ultracut”, stained with 1% Toluidine blue solution for optical microscopy observation. Ultrathin sections 60–90 nm thick were then cut from appropriate areas of the slabs. These ultrathin sections were stained with a saturated solution of uranyl acetate and a 1% solution of lead citrate. A Philips FEI Techni 12 Biotwin transmission electron microscope was used for observation.

B. Periodic arrangement of locomotory cilia

Transmission electron microscopy, applied to the base of the combs of *Beroë cucumis* revealed the periodic arrangement of cilia shown in Fig. 2. The images suggest that the iridescent organs in the comb jellyfish are structured as a two-dimensional photonic-crystal. The refractive index dis-

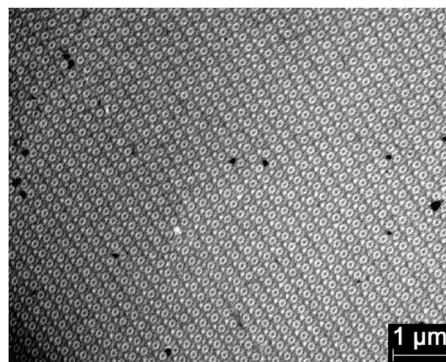


FIG. 2. A section through the comb row of the ctenophore *Beroë cucumis*, showing the structure responsible for the iridescence. The regular packing of the cilia is apparent, each one being found at a node of an orthorhombic lattice. Some of the internal structure of the cilia is visible; from an optical point of view this can be described as a central pair of microtubules (the “central microtubules pair”), here treated as a single unit, which is surrounded by nine other microtubules distributed evenly and at a constant distance from the central microtubules pair.

tribution shows a periodic variation in the cross section, while the known geometry of the cilia suggested a total translational invariance along the orthogonal direction. The structure can be described as a collection of identical cylindrical tubes (“cilia”), composed of smaller rods (“microtubules”); all the cilia and microtubules run parallel to one another. Inside the microtubules, the refractive index is slightly larger than in the space inbetween: the refractive index of the filling tissue is very close to that of salted water ($n_0=1.34$), while the refractive index in the microtubules, though difficult to measure, should not exceed the estimated value $n_r=1.57$. In fact, the exact value of the refractive index of the microtubule is not known. Microtubules are composed of tubulin, dynein, and nexin [9], and, to our knowledge, the refractive index of these substances have not been reported. The estimation used here rests on the fact that this index cannot be less than that of sea water (1.34) and, most probably, cannot exceed the highest refractive index encountered so far in color-producing biological media (1.83 for guanine). The central value 1.57 can be used as an estimation because small variations of this parameter, in the appropriate range, do not significantly impact the optical properties. The model proposed below is then based on these estimations, and we have checked that small variations of these quantities do not alter the quantitative conclusions that can be drawn from these assumed values.

The collection of parallel cilia is highly ordered: a dislocation line (terminated as an empty dot) can even be perceived in the arrangement shown in Fig. 2. The two-dimensional lattice describing this cilial repetition is easily determined from the transmission electron microscope images, as the preparation of the samples was carried out without destroying the coherence of the cilial ordering. As described above, the translation vectors were not of exactly equal lengths, one of them commanding a translation over a distance $d_1=215$ nm and the other defining a slightly shorter move of $d_2=195$ nm. The angle between these translation

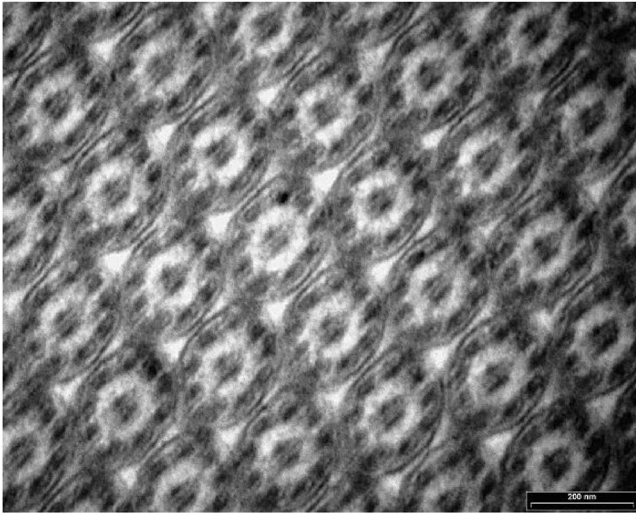


FIG. 3. A transmission electron micrograph of a section through the color-producing structure found in the comb-row of the ctenophore *Beroë cucumis* at a higher magnification than in Fig. 2. The internal structure of the cilia comprises eleven microtubules, but the central pair are fused and were treated as a single entity.

vectors was found to be 77° . Each unit cell contains one cilium, with ten roughly cylindrical internal microtubules, the diameter of which can be estimated to be 40 nm. Among these, we distinguish, in Fig. 3, a central “core”, which, strictly speaking, is composed of a pair of two, linked microtubules, here with a combined diameter of 40 nm. The central pair of microtubules is surrounded, at a constant distance of 73 nm, by nine other, evenly distributed, neighboring microtubules. The direction in which these nine neighbors are found, when viewed from the central core, is exactly the same in all unit cells, an observation that confirms the very strong geometric coherence of the whole structure. This type of cilia structure (known as a “9+2” microtubule arrangement) typical of the vast majority of cilia found throughout the natural world, including those in many other tissue types, such as internal epithelia in vertebrates.

The photonic crystal appears to be a slight distortion of a compact hexagonal lattice (the angle of 77° between the translation vectors would be exactly 60° in a real hexagonal lattice, and d_1 and d_2 would be equal). This distortion could possibly be induced at some stage of the sample preparation, or might be found originally in the living organism. This is particularly difficult to decide with present-state observation tools, in view of the fragility of the samples, out of equilibrium with water. One hint is the observation of a ninefold symmetry in an isolated cilium, which is not an acceptable symmetry for the whole periodic structure. As group theory shows, a ninefold symmetry is incompatible with any of the five existing planar lattices. The somewhat minimally-symmetric oblique structure might plausibly better accommodate this unit cell contents than an exact six-fold symmetric hexagonal structure. For this reason, inferring from the acquired data an exact hexagonal lattice does not seem to be justified, and the slight observed distortion will be maintained in modeling the optical properties of the crystalline structure. It should be noted that the optical properties of the

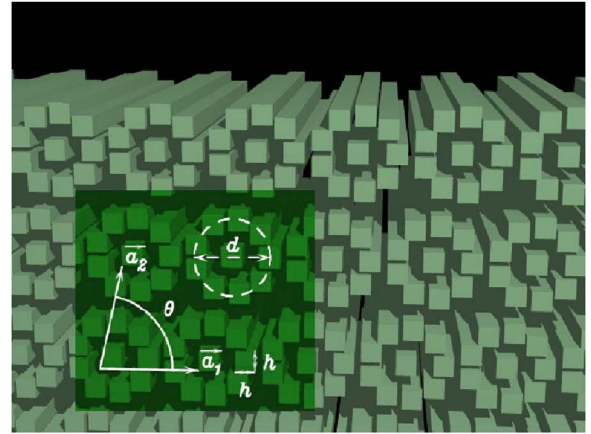


FIG. 4. (Color online) Model for the reflectance of the tightly packed cilia found in the combs of *Beroë cucumis*. The two translation vectors \vec{a}_1 and \vec{a}_2 have the respective lengths $d_1=215$ nm and $d_2=195$ nm, and the angle θ between them is 77° . The diameter d of the high-refractive circle is 73 nm, and the size of the microtubules forming the central pair is $h=40$ nm.

strictly hexagonal lattice will not differ enough from those of the oblique lattice to call into question any of the conclusions drawn here.

III. PHOTONIC-CRYSTAL MODEL AND COMPUTED REFLECTANCE

The optical reverse engineering of the structure found in the ctenophore’s comb rows starts with a slight idealization of the geometry. For *Beroë cucumis*, the structure of the idealized refractive index distribution is given in Fig. 4. The ciliary bundle is essentially a uniform infinite medium with the refractive index of seawater, in which each cilium provides a diffusive refractive index reinforcement. These regions of higher optical density are found along the central axoneme, and on the nine microtubules distributed at 73 nm around it. This distribution is repeated by translation along the vectors \vec{a}_1 and \vec{a}_2 , as described above, to define each cilium in the structure.

This bulk structure is terminated along a surface parallel to the cilia’s axes direction (for lateral exposition to incident light) and the translation vector \vec{a}_1 of length d_1 . Obviously, only entire cilia enter the structure. Other reflecting surfaces exist, which correspond to different reticular planes in the lattice (including the surface containing the vector \vec{a}_2 of length d_2), but due to the deep penetration of the light in this weakly contrasted photonic material, specific surface effects are not expected to be important and changing the surface orientation merely redefines the origin of the incidence and emergence angles. The crystal termination shown in Fig. 4 is then considered generic, and the discussion will be limited to this particular surface orientation.

Even for this quite complicated structure, the reflectance can be calculated, using an “S” transfer-matrix approach, adapting the band-structure computation technique of Pendry [3] to the computation of scattering intensities. For technical reasons, the cylinders have been replaced by prisms with

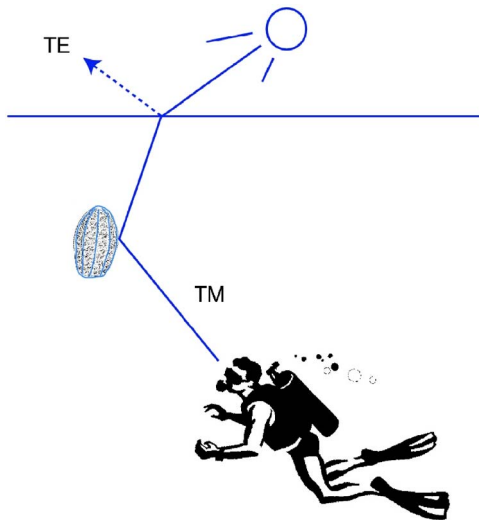


FIG. 5. (Color online) The special illumination situation considered for modeling. The sun, the ctenophore, and the observer are in the same plane, normal to the seawater surface, and the animal is swimming upwards. At an incidence close to the Brewster angle on the sea surface, some transverse-electric light is reflected, while the transverse-magnetic waves are fully transmitted into the sea.

square sections. This approximation has virtually no effect on the calculated reflectance spectrum, because the reflected wavelengths are much larger than the characteristic size of the volumes displaced in the transformation.

Setting up the incident light beam characteristics is another important aspect of these computations. One parameter describes the location, orientation, and state of deformation of the animal body, in relation to the location of the eye of the observer. This parameter is the emergence angle, defined by the exiting light ray and the normal to the surface structure. This emergence angle is actually related to the incident light direction (in the absence of diffraction, specularity is the rule) and, in an ideal situation, any light beam emergent to an observer below the animal arises from some point at the water surface, which can be considered as an extended white illuminant. For an animal which is seen, from below, aiming vertically towards the surface, this gives an incidence-emergence plane which contains the axes of the cilia. The change of location of the animal, and the deformation of the body (leading to a change in orientation of the cilia bundle) produces variations of the emergence and incidence angle. As will be explained below, these incidence angle variations are able to change the dominant wavelength reflected to the observer. In the vertical geometry, where the incident light comes from the sea surface and gets reflected by the animal towards an observer at some greater depth (see Fig. 5), the illumination is maximal if the incidence plane is also the plane containing the sun and the normal to the sea surface. The transverse-magnetic (TM) polarization, in this situation (and especially close to the Brewster incidence angle), dominates the transverse-electric (TE) polarization. However, because of the weak refractive index contrast, this polarization effect will have little impact on the reflectance, even for large incidence angles.

The visible specular reflectance spectra are shown in Fig. 6, for different incidence angles θ and for the incident polar-

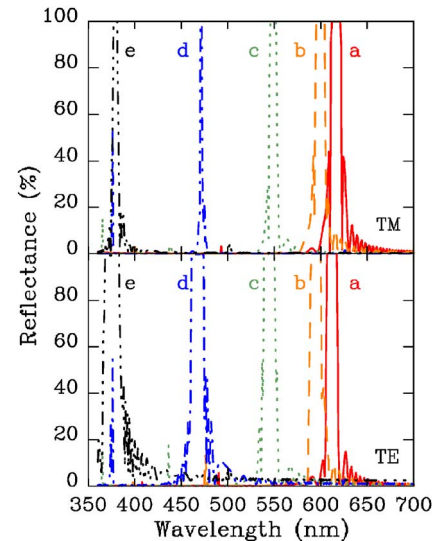


FIG. 6. (Color online) Reflectance of the model structure of the cilia bundle in the comb rows of *Beroë cucumis*, in TM (above) and TE (below) polarizations, for various angles of incidence θ . (a) $\theta = 0^\circ$; (b) $\theta = 15^\circ$; (c) $\theta = 30^\circ$; (d) $\theta = 45^\circ$; (e) $\theta = 60^\circ$.

izations TM and TE. As can be seen, the reflectance is not drastically dependent on the polarization. At normal incidence ($\theta = 0^\circ$), the reflectance is very low for all wavelengths, except in a near-total reflection band centered on $\lambda = 615$ nm, in the red part of the visible range. Then, for increasing incidence angles, this specular reflection band shifts to shorter wavelengths, sweeping the whole visible spectrum (orange for $\theta = 15^\circ$, yellowish green for $\theta = 30^\circ$, blue for $\theta = 45^\circ$). For $\theta = 60^\circ$, the reflection already touches the ultraviolet range. The significance of this result is that, according to the orientation of the photonic-crystal structure with respect to the observer-animal view axis, different visible wavelength will be reflected, assuming that the sea surface behaves as an extended white-light illuminant. The fact that the whole visible range, from red to violet is scanned with moderate angle changes (from normal to about 60° means that the animal motion and deformations easily generate color variability, as observed in the comb jellyfish).

The results provided by this extensive simulation can be understood in terms of a very simple model, based on a one-dimensional photonic-crystal theory, where the presence of a directional gap in the mode frequencies explains the occurrence of total-reflection bands in the reflectance. This theory assumes that the refractive index contrast in the periodic structures is weak (which is obviously true here) and that the structure can be viewed as a simple one-dimensional multilayer, by averaging the refractive index in planes parallel to the structure's surface. This approximation is usually well verified if the incidence is near to normal, because in that configuration, the lateral wavelength of the electromagnetic field is always much larger than the lateral period of the structure. In this approximation, the complicated structure shown in Fig. 4 can be viewed as an homogeneous medium of average refractive index \bar{n} slightly perturbed by the "vertical" distribution of the microtubules. The dispersion relation of light waves propagating in the multilayer structure in this average homogeneous material is

$$\omega = k \frac{c}{\bar{n}}, \quad (1)$$

where k is the norm of the wave vector. This relationship will be modified by the periodic contrast induced by the presence of the microtubules. For waves traveling in periodic media, it is known that only wave numbers which differ by an integer amount of the quantum $2\pi/a$ (where a is the one-dimensional lattice parameter) can hybridize and move to open a frequency gap. This only occurs at the border of the Brillouin zones, when

$$k_z = m \frac{\pi}{a}, \quad (2)$$

(m being an integer: $m=1, 2, 3, \dots$). The normal wave number k_z is actually related to the wave frequency and to the conserved parallel component k_y of the wave traveling through the structure

$$k_z = \sqrt{\left(\bar{n} \frac{\omega}{c}\right)^2 - k_y^2}. \quad (3)$$

If the one-dimensional photonic crystal is terminated by a surface, it is very simple to see a connection between the wave traveling in the structure and an incident wave, because the lateral wave number k_y is conserved in a laterally homogeneous medium. In water (refractive index n_0), with an incidence angle θ , this is

$$k_y = n_0 \frac{\omega}{c} \sin \theta. \quad (4)$$

Finally, using these relations, we can locate the wavelengths where a “multilayer” directional gap occurs. These can be expressed as

$$\lambda = \frac{2a}{m} \sqrt{\bar{n}^2 - n_0^2 \sin^2 \theta}. \quad (5)$$

The integer values of m to be retained are those leading to visible wavelengths, when this is the range of interest. When only one integer value m leads to a visible dominant wavelength λ , the coloration of the multilayer is readily determined from this formula [10].

With the structure discovered in *Beroë cucumis*, this rule produces the following predictions: first, the period a is the length of the unit cell, in the direction normal to the surface, once the refractive index has been laterally averaged. Here, $a = (215 \text{ nm}) \times \sin(77^\circ) = 210 \text{ nm}$. The mean refractive index can be estimated to be 1.47 (somewhat larger than water, but smaller than the axoneme’s index). Only one value is found in the visible range (it corresponds to $m=1$). This explains the simple spectrum found in the more detailed simulation above for the normal incidence, including the location of the reflection band in the red range. We note the lack of a diffracted beam: only the specular reflection is expected. When the angle θ is increased, the effective average index \bar{n} tends to decrease, so that the wavelength is blueshifted. For example, with $\theta=90^\circ$, the above effective index is reduced to 0.91, and the reflected wavelength turns out to be 384 nm. This wavelength is the onset of the visible spectrum on the

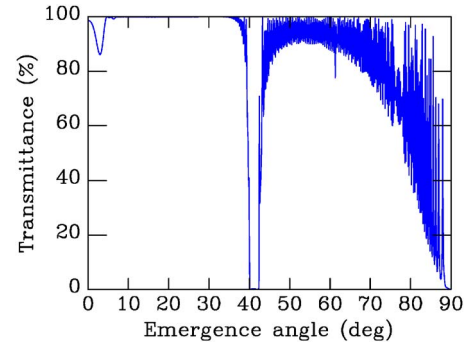


FIG. 7. (Color online) Transmission of the tightly packed cilia at the specific wavelength of 489 nm, which corresponds to the maximal bioluminescence of *Beroë cucumis*. The transmission is nearly perfect for emergence angles below the high-reflection band.

ultraviolet side. This, again, is in perfect agreement with the reflectance properties found with the full numerical simulations. From a physics point of view, the fact that such a crude one-dimensional model agrees so well with the full two-dimensional simulations described earlier means that the parameters which are important to explain the iridescence mechanism of the *Beroë cucumis* structure are, firstly the “vertical” lattice parameter a and, secondly, the mean refractive index, which is related to the volume fraction occupied by the microtubules in the structure. The details of the geometric arrangement of the cilia in a unit cell, and the geometry of their cross section, are subsidiary.

IV. TRANSPARENCY OF THE IRIDESCENT LAYER

In the ctenophore, the tissue bearing the photonic crystal structure is located outside of a bioluminescent organ which emits a rather sharp line at 489 nm, in the bluish-green range. One obvious question arises: what is the filtering effect of this structure on the bioluminescent light transmitted into the water? One answer is shown in Fig. 7, where the transmittance of a thick film of the two-dimensional photonic crystal is calculated at the wavelength of maximal bioluminescence as a function of the angle of incidence (which is also the angle of emergence from the structure). In keeping with what has been described above, the directional gap at 489 nm is found for a direction slightly above 40° . But the most important feature conveyed by this calculation is that the transmission is quasiperfect for angles below this gap. This result can be compared, for instance, with the transmission spectrum shown in Fig. 8, which corresponds to a planar multilayer obtained by displacing the materials in the high-refractive microtubules into a flat layer of thickness 82 nm, the rest of the total period $a=210 \text{ nm}$ being given the refringence of the soft tissue in the cilia. This multilayer conserves the vertical translational invariance and the average refractive index, so that the spectra of Fig. 7 and Fig. 8 are very similar. The transmission of the real two-dimensional structure is an improvement on the already very good transmission of the multilayer. The difference arises because the two-dimensional ciliary packing is less organized than the multilayer stack, so that the more diffuse character of the

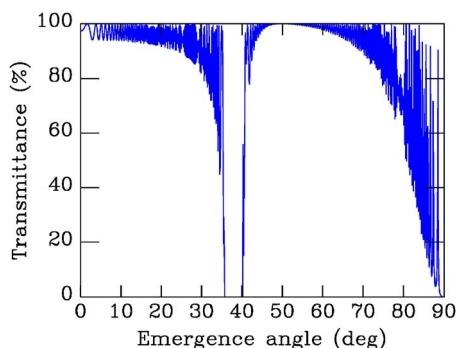


FIG. 8. (Color online) Transmission of a multilayer obtained by reorganizing the material in the cilial structure into a binary periodic planar multilayer with the same period as the original two-dimensional structure. The low transmission gap is found under the same angle as the two-dimensional structure, but the average transmission is slightly weaker, for lower angles.

refractive index distribution avoids the Fabry-Perot oscillations and leads to maximum transparency. This kind of optimization is not found for angles of emergence larger than the gap angle (40°).

It is interesting to see if the structure is, in some sense, optimized for the bioluminescence at 489 nm. Measuring an optimization process raises the question of defining a “target” function which might become maximal for the observed bioluminescence wavelength. We checked the transmission “efficiency”, defined as the average of the angular transmission, weighted for low emergence angles. In more precise words, we consider the efficiency η defined as follows:

$$\eta(\lambda) = \frac{\int_0^{\pi/2} T(\theta, \lambda) e^{-(\theta/\Delta\theta)} d\theta}{\int_0^{\pi/2} e^{-(\theta/\Delta\theta)} d\theta}. \quad (6)$$

The result is shown in Fig. 9, for an emission in a range of 20° around the normal emergence ($\Delta\theta=10^\circ$). The highest values are found very near the observed bioluminescence wavelength $\lambda=489$ nm, but the maximum is found to be very

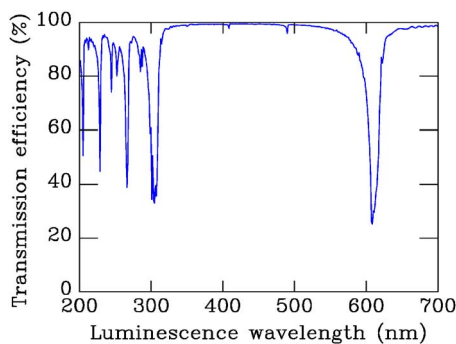


FIG. 9. (Color online) Transmission efficiency of the tightly packed cilia as a function of the luminescence wavelength. The efficiency is measured for emergence angles in the range $\pm\Delta\theta$, where $\Delta\theta=10^\circ$.

flat. With this kind of target function, any optimization process is very difficult, and no definitive conclusion can be drawn at this stage with regard to the adaptation of the structure to the bioluminescence.

V. CONCLUSION

The photonic device which is found in *Beroë cucumis* has at least two well evolved capabilities. It can be viewed as a structured film which simultaneously filters the light in two different ways: in reflection, it provides an exceptionally wide range of iridescence, covering nearly all the visible spectrum, and continuing into the nearest ultraviolet wavelengths; in transmission, it clearly optimizes its transparency in a very wide range of transmission directions, and, in particular, is highly efficient for the specific wavelengths close to the animal’s bioluminescence.

The origin of the iridescence of these animals is the selective reflection of white light by the bundles of cilia which constitute the locomotory organs of the ctenophore. It is difficult to speculate as to the function of this iridescence, since these comparatively simple animals lack image-forming eyes. The iridescence of insects and birds, for instance, is often associated with conspecific recognition signals; it is difficult to propose that such a communication mechanism is in operation here and it seems more likely that the iridescence constitutes either an aversive visual signal to predators or an attractive visual signal to potential prey. Some potential predators and some potential prey of ctenophores do possess sophisticated visual systems, however, pelagic food webs are poorly understood and our knowledge of ctenophoran behavior is similarly scant; there is room here for further biological and, specifically, ethological study.

An interesting aspect of the present case is that iridescence appears on an organ which has another function, namely locomotion, and that it takes place in parallel with another useful optical property, namely transparency. This brings complexity to the evolutionary paths, as very different functions may place competing demands for improvements and, in such a case, the selection process arises from a global optimizing pressure. This, however, does not preclude that some functions can optimize particularly well. If the pressure for their evolution is stronger, or if the variations of these properties do not impact, or impact positively, the performance of the other functions, there is no reason that a specific biological device should not reach an operational perfection.

On more technological grounds, the properties displayed by a layer structured as the iridescent organ of *Beroë cucumis* suggests many interesting applications. We have here a mirror, which is able to select various colors according to its orientation. Combined with micro-electro-mechanical systems, this kind of mirror could be used in color displays, with the advantage of being optically powered by the ambient light. Electroluminescent devices rapidly lose their efficiency if they are used outside, in dazzling sunlight. By contrast, with reflective pixels, very bright incident light could be favorable. Furthermore, due to the fact that the associated structure is also highly transparent, it is conceivable that

these mirrors could be superimposed upon ordinary, electroluminescent pixels, and preserve the device functionality in dark environments.

ACKNOWLEDGMENTS

This work was partly supported by the EU through FP6 BIOPHOT (NEST/Pathfinder) 012915 project, by the EU5 Centre of Excellence ICAI-CT-2000-70029 and by the Inter-University Attraction Pole (IUAP P5/1) on “Quantum-size effects in nanostructured materials” of the Belgian Office for Scientific, Technical, and Cultural Affairs. This work has also been partly supported by the European Regional Development Fund (ERDF) and the Walloon Regional Government under the “PREMIO” INTERREG IIIa project. The

authors acknowledge the use of Namur Interuniversity Scientific Computing Facility (Namur-ISCF), a common project between the Belgian National Fund for Scientific Research (FNRS), and the Facultés Universitaires Notre-Dame de la Paix (FUNDP). V.W. is funded by The Royal Commission for the Exhibition of 1851 and V.L. was supported by the Belgian National Fund for Scientific Research (FNRS). We thank Dr. Tamara Frank and Dr. Edith Widder of Harbor Branch Oceanographic Institute. Thanks are also due to Dr. Steve Haddock of MBARI for identifying the ctenophore and to Jenny Corrigan for technical assistance with the sample preparation. The cruise on which this sample was collected was funded by NSF Grant No. OCE-9730073 to T. M. Frank and E. A. Widder. We thank Dr. Kevin Raskoff, California State University, Monterey Bay, USA, for providing the picture in Fig. 1.

-
- [1] S. H. D. Haddock and J. Case, *Biol. Bull.* **189**(3), 356 (1995).
[2] S. H. D. Haddock and J. Case, *Mar. Biol. (Berlin)* **133**(3), 571 (1999).
[3] J. B. Pendry, *J. Mod. Opt.* **41**, 209 (1994).
[4] G. A. Horridge, *Proc. R. Soc. London, Ser. B* **162**, 351 (1965).
[5] B. A. Afzelius, *J. Biophys. Biochem. Cytol.* **9**, 383 (1961).
[6] G. A. Horridge and B. Mackay, *Q. J. Microsc. Sci.* **105**, 163 (1964).
[7] A. R. Parker, R. C. McPhedran, D. R. McKenzie, L. C. Botten, and N. A. Nicorovici, *Nature (London)* **409**, 36 (2001).
[8] R. C. McPhedran, N. A. Nicorovici, D. R. McKenzie, L. C. Botten, A. R. Parker, and G. W. Rouse, *Aust. J. Chem.* **54**, 247 (2001).
[9] B. Alberts, D. Bray, J. Lewis, M. Raff, K. Roberts, and D. J. Watson, *Molecular Biology of the Cell* (Garland Publishing, Inc., New York, 1994).
[10] R. W. G. Hunt, *Measuring Colour* (Ellis Horward Ltd., London, 1987).